Al-ion Battery Based on Semi-Solid Electrodes for Higher Specific Energy and Lower Cost

*David Muñoz-Torrero, Jesús Palma, Rebeca Marcilla, Edgar Ventosa**

Electrochemical Processses Unit. IMDEA Energy, Parque Tecnológico de Móstoles,

Avda, Ramón de la Sagra 3, 28935 Móstoles, Madrid. Spain.

E-mail: edgar.ventosa@imdea.org

Abstract

Rechargeable aluminum-ion batteries (AIBs) have been intensively studied during the last years. However, its commercialization is still hindered by the relatively high capital cost. Increasing the specific areal capacity (mAh cm^{-2}) by using high mass loading of active material in thick electrodes is an effective strategy to decrease the battery cost. Unfortunately, the high viscosity and low ionic conductivity of the ionic liquid electrolytes prevents the implementation of this strategy. Herein, the use of semi-solid electrodes in AIBs is for the first time proposed to addresses i) the poor wettability related to high viscosity and ii) increase mass transport through thick electrodes limited by the low ionic conductivity. Indeed, specific areal capacities of up 7 mAh cm^{-2} are achieved in this work, compared to 0.5–1.5 mAh cm^{-2} as state-of-the-art. This innovative concept is potentially implementable to advanced material designs to archive improved battery performance in future.

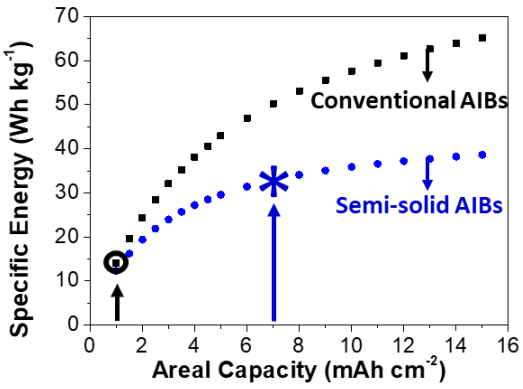

Keywords

Semi-solid electrode, Al-ion battery, enhanced mass transport, electrode porosity, high mass loading electrodes

Rechargeable Aluminum-ion batteries (AIBs) has recently been attracting the attention of the scientific community due to the appealing features of Al metal, i.e. excellent theoretical volumetric and gravimetric capacities (8.04 Ah cm^{-3} and 2.05 Ah g^{-1}, respectively), low acquisition cost, high abundance, safety and non-toxicity.[1] AIBs comprise of a metallic aluminum as anode and negative current collector, a chloroaluminate ionic liquid as electrolyte ($AlCl_3$:EMImCl with a molar ratio, *r*, higher than one), an Al-insertion cathode material such as polymers,[2] vanadium oxides,[3] or graphitic materials amongst others,[4–6] and a positive current collector such as tungsten (W),[6] molybdenum (Mo),[5] and more recently, titanium nitride (TiN)[7] and GDL-based on carbon.[8] AIBs offer longer cycle life, higher specific power and increased safety, compared to state-of-the-art Li-ion batteries, but lower energy density since it is not an Al-ion rocking-chair.[6,9] Thus, stationary energy storage appears to be the most suitable application for AIBs. On the other hand, capital cost (USD kWh^{-1}) is at the moment too high.[9] There are three strategies to decrease this capital cost: i) the use of cheaper materials, ii) the increase of the energy density, iii) the increase of the specific areal capacity to decrease the content of inactive elements. While intensive efforts are being devoted to the two former options, surprisingly the third strategy has been neglected. **Figure 1a** shows the strong influence of the areal capacity in the battery cost that was calculated considering the acquisition cost of the most widely used current collectors for AIBs (Mo and W).[8] As the areal capacity increases, the total area of battery decreases requiring less amount of inactive materials, e.g. current collector and separator. However, the vast majority of report in AIBs demonstrated areal capacities lower than 0.6 mAh cm^{-2}.[4,10] As summarized in **Figure S1**, only some recent reports published by Kovalenko´s group achieved a value closed to 1.5 mAh cm^{-2}.[6,11] Although further increase in areal capacity is greatly desired, it is challenging to exceed those values since the high viscosity and low ionic conductivity of ionic liquid electrolyte leads to poor mass transport

of ions, described by the effective diffusion coefficient, through thick electrodes (ionic resistance for $AlCl_4^-$, $R_{AlCl_4^-}$, **Figure 1b**). The transport of $AlCl_4^-$ ions should be facilitated by increasing the effective diffusion to achieve high specific capacities in thicker electrodes (higher areal capacities). The effective diffusion coefficient (D_{eff}) that describes diffusion through the pore space of porous media is related to the porosity (ε) and the tortuosity (τ) of the electrodes following this equation: $D_{eff} = \frac{\varepsilon}{\tau} D_o$, where D_o is the diffusion coefficient of $AlCl_4^-$ ion in the bulk electrolyte. Therefore, the effective diffusion coefficient might be improved by increasing the porosity and/or decreasing the tortuosity. In addition, the necessary use of binder in conventional electrodes, increases the tortuosity hindering diffusion of ions.[12] In fact, the porosity also influences the tortuosity since the pathways for ions become more tortuous as porosity decreases. In this work, we propose for the first time the use of semi-solid cathodes with improved effective diffusion coefficient instead of traditional solid cathodes. Semi-solid electrodes are dense slurries that are made of graphite powder and electrolyte in absence of binder. These slurries can achieve electrical percolation having a higher porosity than conventional electrodes, which allows these electrodes to have enhanced transport of ions. This concept can then be exploited to achieve a breakthrough in AIBs by demonstrating relevant areal capacity values at relatively high C-rate (0.2 C – 2 C), which are required to make AIBs more economically competitive, using conventional cathode materials. The use of semi-solid electrode not only contributes to decreasing the battery cost by increasing the areal capacity, but it also facilitates some manufacturing process issues related AIBs. The low wettability of viscous electrolytes, e.g. concentrated electrolytes and ionic liquids, makes the manufacturing process more expensive since ensuring proper wetting slow down the production. The electrolyte is already present in the semi-solid electrode so that poor wetting of porous electrode during manufacturing can be potentially overcome.

Several mixtures of electrolyte and graphite powder (SGP) were prepared to develop a semi-solid cathode (binder-free) with a high electrical percolation by following the procedure described in Section 2 of the ESI. It should be noted that conventional materials were selected to show the benefits of this innovative concept without additional improvement originated from the active material itself. A separator-free symmetrical cell (**Figure S2**) was used for this purpose applying electrochemical impedance spectroscopy (**Figure S3**). The results indicated that the mixture containing 28 vol.% of graphite powder (72 % electrode porosity) showed the lowest resistance so that this mixture was selected for subsequent tests. The electrical conductivity of the slurries was 0.13 S cm^{-1} including 2 interfaces current collector – semi-solid electrode (Section 3 of the ESI) Thus, the Ohmic resistance at the highest current density (4 mA cm^{-2}) would contribute with up to 3 – 12 mV for a thickness range between 1-mm and 4-mm. The implementation of semi-solid electrodes for AIBs required the development of a new battery cell configuration (**Figure 1c)**. An Al foil and an Al mesh were used as current collector and anode for ensuring that the positive electrode is the capacity limiting electrode (**Figure S4**). A picture of a semi-solid electrode held by two fingers (**Figure 1d**) shows the high viscosity of these type of electrodes.

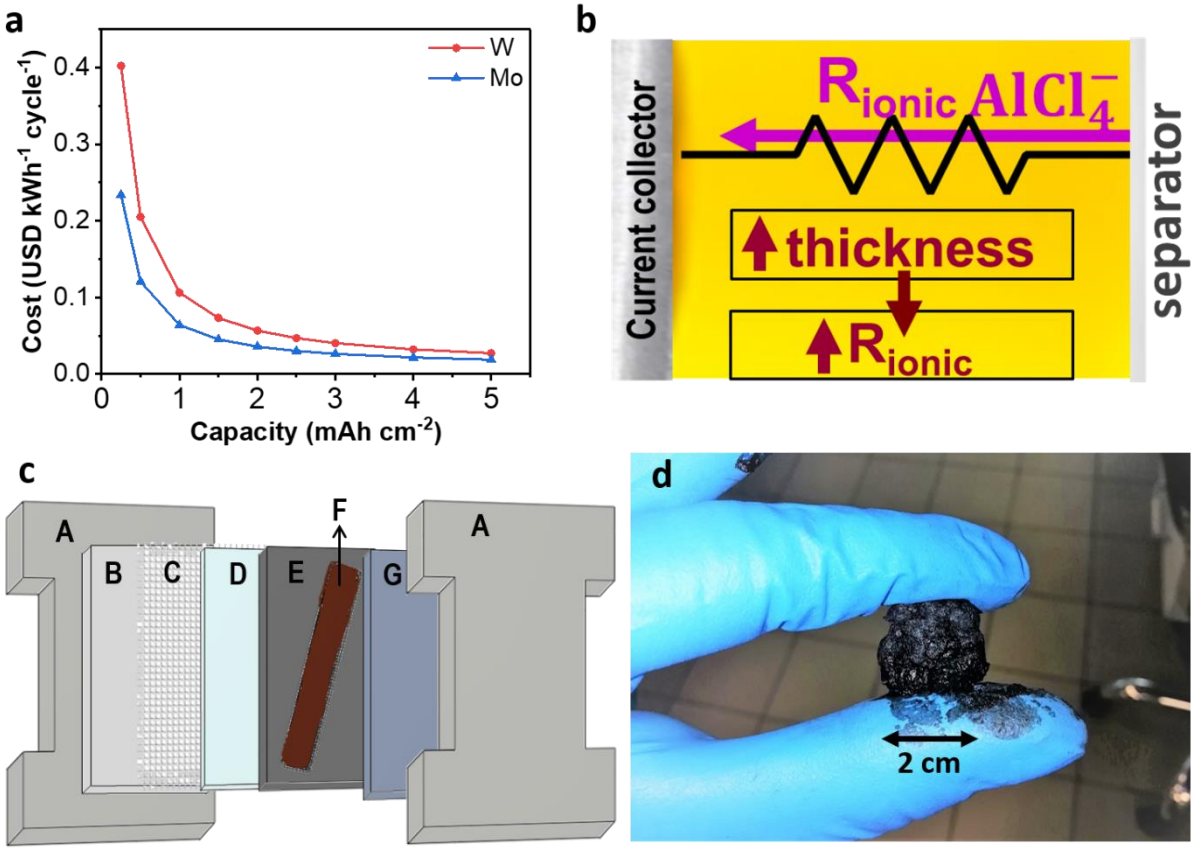

Figure 1.(a) Capital cost per cycle (USD kWh^{-1} $cycle^{-1}$) for AIBs *vs* areal capacity (mAh cm^{-2}). Cycle life taken ref. 13. (**b)** Dependence of ionic resistance *vs* thickness. (**c)** Electrochemical cell designed: A–Teflon plates, B–Al foil, C–Al mesh, D–separator, E–Viton gasket, F–Semi-solid cathode, G–W current collector. And (**d**) Picture of a semi-solid electrode hold by the 2 fingers.

First, the performance of high-areal-capacity semi-solid and conventional electrodes was evaluated by assembling cells using 1-mm-thick semi-solid and conventional cathodes (**Figure 2a**). It should be noted that the uneven distribution of overpotentials through thick electrodes prevents observing the characteristic two plateaus for graphitic cathodes in the voltage profile of AIBs.[8] The areal capacity of the semi-solid (76 $mg_{graphite}$ cm^{-2}) and conventional cathode (84$mg_{graphite}$ cm^{-2}) were 3.35 mAh cm^{-2} and 1.93 mAh cm^{-2}, respectively. The use of semi-solid electrodes in AIBs not only increased the areal capacity but also the utilization rate of active

material (44 mAh g^{-1} vs. 23 mAh g^{-1} at 4mA cm^{-2}). Compared to conventional electrodes, the lower overpotential observed for semi-solid electrodes is likely due to an enhanced mass transport of ions through thick electrode and reveals a good electrical contact for the semi-solid electrodes. Indeed, the Warburg coefficients (σ_W) (**Figure 2b)** extracted from electrochemical impedance spectroscopy measurements confirmed that effective diffusion coefficient in semi-solid electrodes is 1.8 times higher than that in conventional electrodes (see Section 6 in the ESI) resulting in batteries with lower overpotentials as observed in **Figure 2a**. Note that measurements were conducted at 50 % SOC for thick electrode (4 mm) to ensure mass transport limitation.

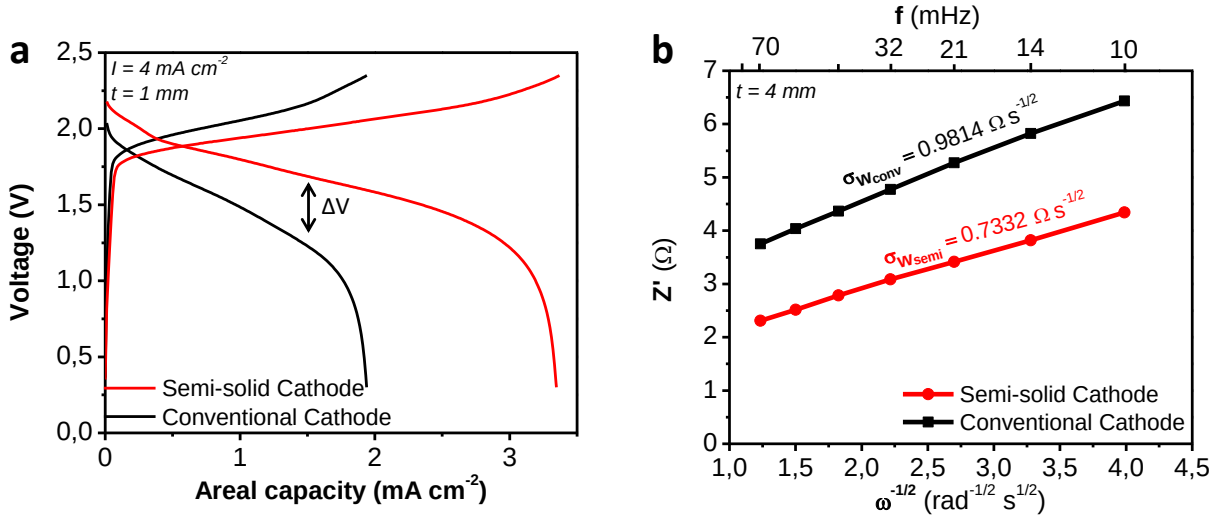

Figure 2. (**a**) Voltage profile for battery cells using conventional and semi-solid electrodes (synthetic graphite powder). Thickness of 1 mm at 4 mA cm^{-2} in a volatge range of 0.3–2.35 V. (**b**) Estimatation of Warburg coeficients for conventional and semi-solid electrodefor a thickness of 4 mm at 50% of SOC.

Thick semi-solid cathodes (1 mm) showed good capacity retention with the C-rate. Between 0.25 C (1 mA cm^{-2}) and 1.25 C (4 mA cm^{-2}), the overpotential did not increase significantly (**Figure**

3a) enabling a capacity retention of 85 % (**Figure 3b**). In all cases, the areal capacities (3.35, 3.61, 3.76 and 3.89 mAh cm^{-2} for 4, 3, 2 and 1 mA cm^{-2}, respectively) are several times higher than the values reported in literature (0.5–1.5 mAh cm^{-2}).In addition, the specific capacity that relates to the utilization rate of graphite was 51.9 mAh g^{-1} at 1 mA cm^{-2},which is closed to the average value obtained for conventional electrodes containing this graphitic material (≈63 mAh g^{-1}).[8] Similarly to conventional electrodes, the utilization rate of AIBs using semi-solid cathodes decreased with increasing thickness (**Figure S5** and **S6**). However, compared to conventional electrodes with similar areal capacity, the utilization rate for semi-solid electrodes was in all cases 30 -80 % higher. For instance, although the areal capacity for 4-mm conventional electrodes is 6 mAh cm^{-2} (Figure S6), the utilization rate drops down to 20 mAh g^{-1} (Figure S5), compared to the 7 mAh cm-2 and 51 mAh g-1 for semi-solid electrode. In terms of specific power, 1-mm thick semi-solid cathodes operating at a power of *ca.* 70 W m^{-2} (4 mA cm^{-2}) delivered a specific power of 95 W kg^{-1} and a specific capacity of 45 mAh g^{-1} (Figure 3b and S5). On the other hand, 1-mm thick conventional cathodes operating at *ca.* 60 W m^{-2} delivered a specific power of 80 W kg^{-1} and a specific capacity of 25 mAh g^{-1} (Figure S5). The best compromise between areal capacity, utilization rate and current density needs to be found for a specific application of AIBs. In terms of cycle life, AIBs using semi-solid electrodes were able to operate for 500 cycles and 790 hours retaining >75 % of its initial capacity (**Figure 3c**) while maintaining a Coulombic and energy efficiency of >99.5 % and >78 %, respectively, at 1.2 C (4 mA cm^{-2}), which rules out sedimentation of active material.

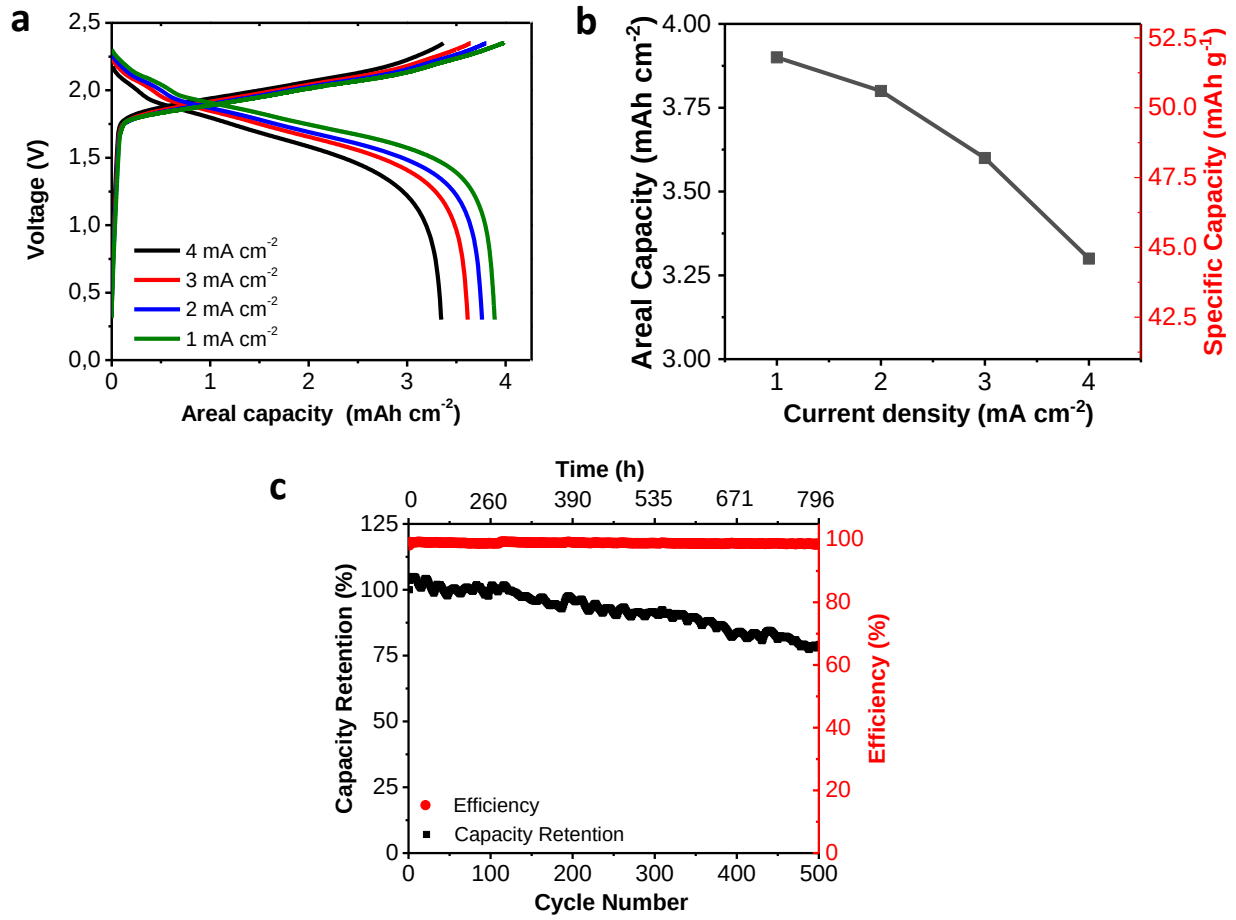

Figure 3. (**a**) Galvanostatic charge-discharge cycles at different currents (1, 2, 3 and 4 mA cm^{-2}) in a voltage range of 0.2–2.35 V.(**b**) Areal capacity and specific capacity for different applied current densities. (**c**) Capacity retention and Coulombic efficiency at 4 mA cm^{-2}. Electrode thickness of 1 mm (76 $mg_{graphite}$ cm^{-2}).

The versatility of the semi-solid AIBs was demonstrated by implementing the concept to other graphitic cathode materials. Synthetic graphite powder (SGP), synthetic graphite flakes (SGF) and mixtures of these two graphites were evaluated as active materials for the cathode of semi-solid AIBs. Textural properties, e.g. differences in specific surface area,[14,15] particle size and particle shape play an important role in the porosity and tortuosity of the resulting semi-solid electrodes. The use of SGF enabled the preparation of slurries with lower porosity (57 %) than that obtained

with SGP (72 %). The higher content of active material for SGF (149 $mg_{graphite}$ cm^{-2}) compared to SGP (76 $mg_{graphite}$ cm^{-2}) for a 1-mm semi-solid electrode resulted in a larger areal capacity of 5.5 mAh cm^{-2} (**Figure 4**). On the other hand, the utilization rate decreased from 52 mAh g^{-1} to 37 mAh g^{-1} for SGP and SGF, respectively. This points out a detrimental effect in the mass transport of ions through the electrode in the case of SGF-based semi-solid electrodes which is likely due to the combination of two factors: i) higher through-plane tortuosity due to graphite flakes alignment that has been shown for conventional Li-ion battery electrodes[16,17]and ii) lower electrode porosity (57 % vs. 72 %). To rule out the former factor, a mixture of graphitic materials with low content of SGP (95 % SGF + 5 % SGP) was prepared in an attempt to decrease the tortuosity expected for pure flake-based electrodes while maintaining a comparable electrode porosity. Since the electrode porosity (58 % and 46 wt.% of electrolyte) of the battery containing 95 % SGF + 5 % SGP was very similar to that (57 %) containing 100 % SGF, the differences in the electrochemical performance between these two cells can be attributed to a decrease in tortuosity promoted by the addition of spherical graphite particles to the flake-based semi-solid electrode. Indeed, the semi-solid battery containing a mixture of active materials delivered excellent performance in terms of mass loading of active material (137 $mg_{graphite}$ cm^{-2}), electrode porosity (58 %), amount of electrolyte (46 wt.%), utilization rate (specific capacity of 51 mAh g^{-1}), specific capacity of the cathode including the mass of electrolyte (28 mAh $g^{-1}_{c+electrolyte}$) and areal capacity (7 mAh cm^{-2}). On the other hand, the utilization rate (20 mAh g^{-1}) and specific capacity of the cathode including the mass of electrolyte (13 mAh $g^{-1}_{c+electrolyte}$) was drastically lower for conventional electrode (34 wt.% of electrolyte) of similar areal capacity (6 mAh cm^{-2}). In addition, the cost breakdown (Section 9 in ESI) shows that the contribution of the electrolyte increases for semi-

solid based batteries, which should benefit from the significant advances in the production cost of ionic liquids.

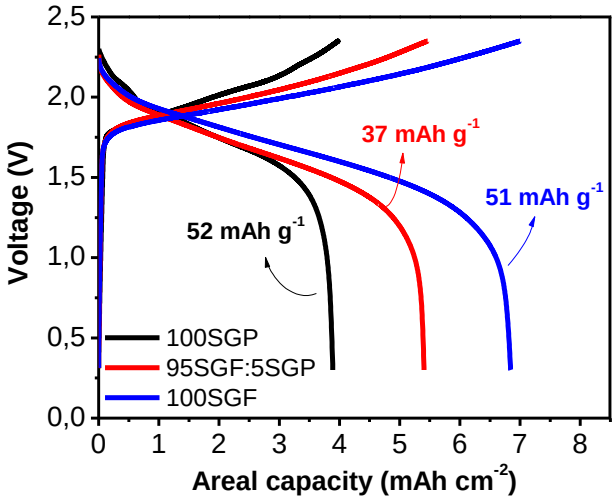

Figure 4. Galvanostatic voltage profiles for 100SGP (black), 100SGF (red) and 95SGF:5SGP (blue) at 1 mA cm^{-2} in the voltage range of 0.2–2.35 V for 1-mm semi-solid electrodes.

In terms of specific energy and energy density, the penalty related to the higher electrode porosity is compensated by the higher areal capacity and the lower amount of inactive materials. **Figure 5a** and **5b** shows the evolution of specific energy and energy density, respectively, with the areal capacity for two electrode porosities (45 and 58 vol%). In terms of specific energy, the increase in areal capacity from 1 mAh cm^{-2} to 7 mAh cm^{-2} outweighs the effect of the increase in electrode porosity from 45 % to 58 vol% resulting in a 2-fold increase in the specific energy for semi-solid AIBs. On the other hand, the effects of the changes in area capacity and electrode porosity cancel each other out for the energy density leading to similar values for AIBs based on both conventional and semi-solid electrodes.

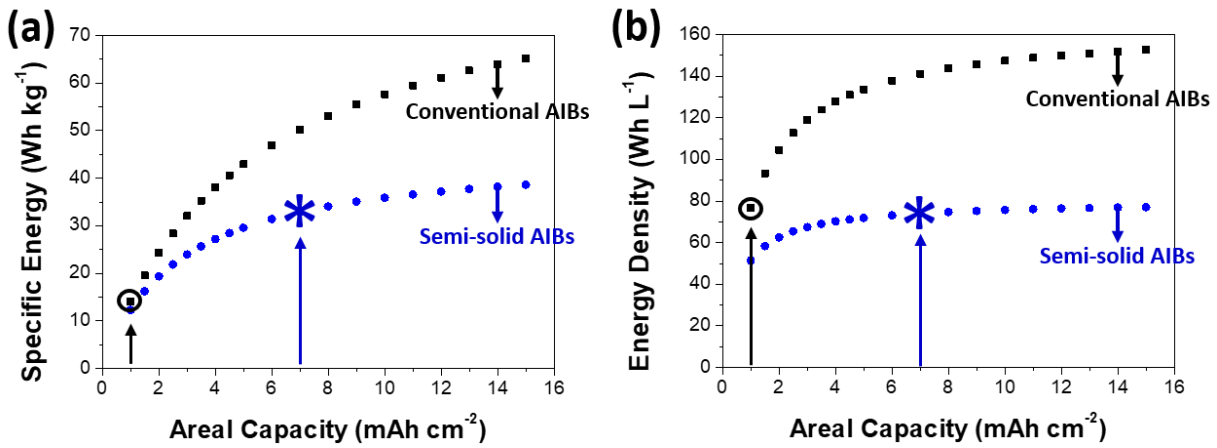

Figure 5. Evaluation of **(a)** specific energy and **(b)** energy density with the areal capacity of AIBs for two electrode porosities: 45 vol% (black squares – conventional electrodes) and 58 vol% (blue circles – semi-solid electrodes). The values were calculating for a thickness of 50 µm for the Al and W current collectors and a specific capacity of 80 and 50 mAh g^{-1} for conventional and semi-solid electrodes, respectively. An electrode porosity of 45 vol% and 58 vol% are used for conventional and semi-solid electrodes, respectively. It should be noted that 1 mAh cm^{-2} is considered as state-of-the-art value for conventional AIBs while a value of 7 mAh cm^{-2} is demonstrated in this work.

In conclusion, the specific areal capacity is a critical battery parameter for the commercial development of Al-ion batteries since it has a tremendous impact on the battery cost. Due to the high viscosity and low ionic conductivity of employed ionic liquids, relevant values of areal capacity are challenging to be achieved using conventional battery electrodes. On the one hand, issues of poor wettability related to viscous electrolytes can be overcome by the use of semi-solid cathodes. On the other hand, the mass transport of ions that limits the maximum areal capacity is increased by using semi-solid electrodes. In this work, the increased mass transport (at least 1.8 times) enable the demonstration of Al-ion batteries with high areal capacities of up to 7 mAh cm-

^{2} at relatively high C-rate (0.2 C – 2 C), compared to 0.5 – 1.5 mAh cm^{-2} as state-of-the-art, while maintaining a good utilization rate (51 mAh g^{-1}) and electrode porosity (58 %). The versatility of the innovative concept is demonstrated by implementing it to two different graphitic active materials, but easily transferred to advanced material designs. This proof of concept for semi-solid Al-ion batteries represents a breakthrough for the commercialization of this technology.

ASSOCIATED CONTENT

Supporting Information.

The supporting information is available and includes the following sections: **Section 1.** Areal capacity in Al-ion batteries: state of the art, **Section 2.** Experimental section, **Section 3.** Optimization of slurry, **Section 4.** Negative electrode (anode) for high areal capacities, **Section 5.** Utilization rate of active material, **Section 6.** Estimation of ratio between effective diffusion coefficients, **Section 7.** Molar ratio of the electrolyte. **Section 8**. Energy density and specific energy calculation. **Section 9.** Cost breakdown for conventional and semi-solid electrodes

Notes

The authors declare no competing financial interest.

ACKNOWLEDGMENT

The authors acknowledge the financialsupport by the Spanish Government (MINECO) through the Research Challenges Programme (Grant RTI2018-099228-A-I00) as well as the Comunidad de Madrid through the Talent Attraction programme (2017-T1/AMB-5190).

REFERENCES

(1) Elia, G. A.; Marquardt, K.; Hoeppner, K.; Fantini, S.; Lin, R.; Knipping, E.; Peters, W.; Drillet, J.; Passerini, S. An Overview and Future Perspectives of Aluminum Batteries. *Adv. Mater.* **2016**, *28* (36), 7564–7579. https://doi.org/10.1002/adma.201601357.

(2) Walter, M.; Kravchyk, K. V.; Böfer, C.; Widmer, R.; Kovalenko, M. V. Polypyrenes as High-Performance Cathode Materials for Aluminum Batteries. *Adv. Mater.* **2018**, *30* (15), 1–6. https://doi.org/10.1002/adma.201705644.

(3) Jayaprakash, N.; Das, S. K.; Archer, L. A. The Rechargeable Aluminum-Ion Battery. *Chem. Commun.* **2011**, *47* (47), 12610–12612. https://doi.org/10.1039/c1cc15779e.

(4) Lin, M.-C.; Gong, M.; Lu, B.; Wu, Y.; Wang, D.-Y.; Guan, M.; Angell, M.; Chen, C.; Yang, J.; Hwang, B.-J.; Dai, H. An Ultrafast Rechargeable Aluminium-Ion Battery. *Nature* **2015**, *520* (7547), 324–328. https://doi.org/10.1038/nature14340.

(5) Sun, H.; Wang, W.; Yu, Z.; Yuan, Y.; Wang, S.; Jiao, S. A New Aluminium-Ion Battery with High Voltage, High Safety and Low Cost. *Chem. Commun.* **2015**, *51* (59), 11892–11895. https://doi.org/10.1039/C5CC00542F.

(6) Kravchyk, K. V.; Wang, S.; Piveteau, L.; Kovalenko, M. V. Efficient Aluminum Chloride-Natural Graphite Battery. *Chem. Mater.* **2017**, *29* (10), 4484–4492. https://doi.org/10.1021/acs.chemmater.7b01060.

(7) Wang, S.; Kravchyk, K. V.; Filippin, A. N.; Müller, U.; Tiwari, A. N.; Buecheler, S.; Bodnarchuk, M. I.; Kovalenko, M. V. Aluminum Chloride-Graphite Batteries with Flexible Current Collectors Prepared from Earth-Abundant Elements. *Adv. Sci.* **2018**, *5* (4), 1–6.

https://doi.org/10.1002/advs.201700712.

(8) Muñoz-Torrero, D.; Anderson, M.; Palma, J.; Marcilla, R.; Ventosa, E. Unexpected Contribution of Current Collector to the Cost of Rechargeable Al-Ion Batteries. *ChemElectroChem* **2019**, *6* (10), 2766–2770. https://doi.org/10.1002/celc.201900679.

(9) Muñoz-Torrero, D.; Palma, J.; Marcilla, R.; Ventosa, E. A Critical Perspective on Rechargeable Al-Ion Battery Technology. *Dalt. Trans.* **2019**, *48* (27), 9906–9911. https://doi.org/10.1039/C9DT02132A.

(10) Wang, D.-Y.; Wei, C.-Y.; Lin, M.-C.; Pan, C.-J.; Chou, H.-L.; Chen, H.-A.; Gong, M.; Wu, Y.; Yuan, C.; Angell, M.; Hsieh,Y.-J.; Chen, Y.-J.; Wen, C.-Y.; Hwang, B.-Y.; Chen, C.-C.; Dai, H. Advanced Rechargeable Aluminium Ion Battery with a High-Quality Natural Graphite Cathode. *Nat. Commun.* **2017**, *8*, 14283.

(11) Wang, S.; Kravchyk, K. V.; Krumeich, F.; Kovalenko, M. V. Kish Graphite Flakes as a Cathode Material for an Aluminum Chloride–Graphite Battery. *ACS Appl. Mater. Interfaces* **2017**, *9* (34), 28478–28485. https://doi.org/10.1021/acsami.7b07499.

(12) Landesfeind, J.; Eldiven, A.; Gasteiger, H. A. Influence of the Binder on Lithium Ion Battery Electrode Tortuosity and Performance. *J. Electrochem. Soc.* **2018**, *165* (5), A1122–A1128. https://doi.org/10.1149/2.0971805jes.

(13) Pan, C.-J.; Yuan, C.; Zhu, G.; Zhang, Q.; Huang, C.-J.; Lin, M.-C.; Angell, M.; Hwang, B.-J.; Kaghazchi, P.; Dai, H. An Operando X-Ray Diffraction Study of Chloroaluminate Anion-Graphite Intercalation in Aluminum Batteries. *Proc. Natl. Acad. Sci.* **2018**, *115* (22), 5670–5675. https://doi.org/10.1073/pnas.1803576115.

(14) Wolf, M.; Fischer, N.; Claeys, M. Preparation of Isolated Co 3 O 4 and Fcc-Co Crystallites in the Nanometre Range Employing Exfoliated Graphite as Novel Support Material . *Nanoscale Adv.* **2019**, *1* (8), 2910–2923. https://doi.org/10.1039/c9na00291j.

(15) Www.Imerys-Graphite-and-Carbon.Com. IMERYS Graphite & Carbon (Accessed October 02, 2019).

(16) Ebner, M.; Wood, V. Tool for Tortuosity Estimation in Lithium Ion Battery Porous Electrodes. *J. Electrochem. Soc.* **2015**, *162* (2), A3064–A3070. https://doi.org/10.1149/2.0111502jes.

(17) Ebner, M.; Chung, D.-W.; García, R. E.; Wood, V. Tortuosity Anisotropy in Lithium-Ion Battery Electrodes. *Adv. Energy Mater.* **2014**, *4* (5), 1301278. https://doi.org/10.1002/aenm.201301278.